Acta Crystallographica Section A
Foundations of Crystallography
ISSN 0108-7673

Received 9 March 2010
Accepted 9 April 2010

Interbranch transient beating of X-ray intensities in deformed crystals

M. Shevchenko

Solid State Theory, Institute for Metal Physics, Vernadsky 36, Kiev 03142, Ukraine. Correspondence e-mail: mishevch@yahoo.com

X-ray dynamical diffraction in a deformed crystal is studied using the interbranch resonance concept. It is shown that appreciable beating of the X-ray intensities may be induced by a lattice distortion that produces interbranch transformations of the local dispersion surface. In X-ray plane-wave topography, this effect may be observed as interference fringes arising around the kinematical image of a defect. It is predicted that such interbranch fringes can be induced by edge dislocations.

1. Introduction

X-ray studies of new materials used in modern technologies and advanced applications often run into serious difficulties due to strong deformation of the crystals. For example, appreciable lattice distortions may be caused by defects appearing in a crystal during the growth process, or may be due to specific manipulations of a sample. Strong deformations induce intense interbranch scattering (Penning, 1966; Authier, 1967). The X-ray diffraction problem may be analytically solved only for some models of strain distribution (Authier, 2005). However, the solutions have a very sophisticated form that considerably complicates their practical utilization. Therefore, numerical calculations of the X-ray intensities have to be carried out in most cases.

It should be noted that activation of interbranch scattering also leads to drastic changes in the dispersion properties of the X-ray wavefields predicted by the concept of the local dispersion surface (Penning & Polder, 1961). The conditions of applicability of this concept for different degrees of deformation were studied by Balibar & Malgrange (1975). By building the crystal wave packets, it was established that the criterion for the concept of the local dispersion surface becoming inapplicable coincides with the criterion of validity of the eikonal approximation of X-ray dynamical theory, obtained by Authier & Balibar (1970).

For investigation of the X-ray interbranch scattering by a highly deformed crystal, the interbranch resonance concept was elaborated in the eikonal representation of X-ray dynamical theory (Shevchenko, 2005). According to the concept, the local dispersion surface for the given polarization consists of four sheets which are formed due to the interbranch splitting of the pair of branches corresponding to a misoriented locally perfect crystal. One of the important parameters of this theory is the interbranch extinction length $\Lambda_g(z_0) = 4\pi^2/[\xi_g \mathbf{g}\,\mathbf{u}''(z_0)]$, such that z_0 is the point where the Bragg condition is locally satisfied and ξ_g, $\mathbf{g}$ and $\mathbf{u}(z)$ are the conventional X-ray extinction length, the diffraction vector and the displacement field, which depends on the depth in the crystal, respectively. The inverse value $k_\Lambda(z_0) = 1/\Lambda_g(z_0)$ determines the interbranch contribution to the resonance splitting of the dispersion surface at the point z_0. As shown by the results of the theory, the interbranch splitting must be taken into account when the interbranch contribution is greater than (or equals) the into-a-branch contribution. In this case, the following condition should be fulfilled:

$$k_\Lambda(z_0) \geq 1/\xi_g. \qquad (1)$$

[It is clear that the into-a-branch process will prevail over the interbranch scattering when condition (1) is violated.] In this work, we assume that the gradients of deformation are considerably greater than the values corresponding to the eikonal approximation of X-ray dynamical theory. At the same time, we suppose that gradients are not so large that the value $k_\Lambda(z_0)$ is of the order of $1/\xi_g$. In this connection, we will analyze the correlation between the degree of deformation and the intensities of the transmitted and diffracted waves. Owing to the resonance character of the interbranch splitting, one can hope that the splitting effect may prominently manifest itself in the X-ray intensities related to the deformation satisfying condition (1). Moreover, we will extend the considerations to the case of a long-range strain field caused by a single dislocation. We will examine this point in detail assuming an edge dislocation.

2. Oscillations of the transmitted and diffracted intensities excited by a lattice distortion

Assuming that the strain field depends on the depth in the crystal, Takagi's equations for amplitudes of the transmitted and diffracted waves $D_{0,g}$ have the following form in the case of symmetrical Laue diffraction:

$$\frac{\mathrm{d}^2 D_{0,g}(z)}{\mathrm{d}z^2} + \left\{\left[\frac{\pi^2}{\xi_g^2} + q^2(z)\right] \pm \frac{i}{2}\mathbf{g}\frac{\mathrm{d}^2\mathbf{u}(z)}{\mathrm{d}z^2}\right\} D_{0,g}(z) = 0, \qquad (2)$$

where $q(z) = [s + \mathbf{g}\,\mathrm{d}\mathbf{u}(z)/\mathrm{d}z]/2$ and s is the departure from Bragg's law of the incident wave. It is necessary to remark that the amplitudes $D_{0,g}(z)$ are determined up to the phase factor $\exp\{i\int q(z)\,\mathrm{d}z\}$. This factor does not contribute to the X-ray intensities and, therefore, it can be omitted. It is worth noting that the limit of the validity of the eikonal approximation of X-ray dynamical theory can be directly deduced from equations (2). For this purpose, it is necessary to compare the first extinction term in the square brackets and the last gradient term in the braces, which must be small for a weak deformation. Thus, we can obtain the following estimation:

$$\frac{\pi^2}{\xi_g^2} \gg \frac{1}{2}\left|\mathbf{g}\frac{\mathrm{d}^2\mathbf{u}(z)}{\mathrm{d}z^2}\right|. \qquad (3)$$

Condition (3) is the criterion of the validity of the eikonal approximation. It is equivalent to saying that the deformation of the lattice over a unit distance is much smaller than a rotation of the order of the width of the rocking curve over a distance equal to the *Pendellösung* distance ξ_g (Authier & Balibar, 1970). On the other hand, the gradient of deformation satisfying condition (1) considerably exceeds the gradients associated with the eikonal limit. This means that the conventional *Pendellösung* beating inherent to both a perfect and a slightly deformed crystal will be absent for the gradient corresponding to equation (1). Nevertheless, taking into account that condition (1) is still associated with the X-ray dynamical diffraction, one can hope that it may determine appreciable dynamical effects which are due to the lattice distortions. In this connection, we will analyze the transmitted and diffracted intensities calculated with the help of the numerical solution of Takagi's equations.

Moreover, we will be interested in applying our considerations to the case of a distortion induced by a defect located inside the crystal. The deformation will increase sharply with the depth z on approaching the defect. Taking this into account, we will approximate the lattice distortion by the increasing exponential $\mathbf{u}(z) = \mathbf{u}_0\exp\{z/l\}$, where $\mathbf{u}_0$ and l are the amplitude of the deformation and the characteristic depth specifying its increment, respectively. Clearly, by varying the parameters $\mathbf{u}_0$ and l, it is possible to change the steepness of the strain distribution and, consequently, to model the different kinds of defects.

Using the resonance condition (1), one can determine the deformation corresponding to the interbranch splitting of the local dispersion surface. If we put $z_0 = 0$ in condition (1), we get

$$k_\Lambda(0) = \varepsilon/(2\xi_g) \geq 1/\xi_g, \qquad (4)$$

where $\varepsilon = \mathbf{g}\,\mathbf{u}_0\xi_g^2/(2\pi^2 l^2)$. Obviously, relation (4) is equivalent to the condition $\varepsilon/2 \geq 1$, which determines the resonance value ε. Condition (4) is strongly satisfied everywhere in the deformed region of the crystal and, moreover, it can also be considered as the threshold relation which separates the influences of the into-a-branch and interbranch contributions on the dispersion properties of the X-ray wavefields. Bearing this in mind, we will calculate the X-ray intensities for the deformations $\varepsilon = 2$ and $\varepsilon = 4$, which satisfy condition (1), and deformation $\varepsilon = 1$, satisfying the opposite inequality $\varepsilon/2 < 1$. The curves corresponding to these deformations are plotted in Fig. 1. [In all cases, it is also assumed that the value $\xi_g/(\pi l) = 2$ and the dimensionless departure $\omega = s\xi_g/(2\pi) = -2$.]

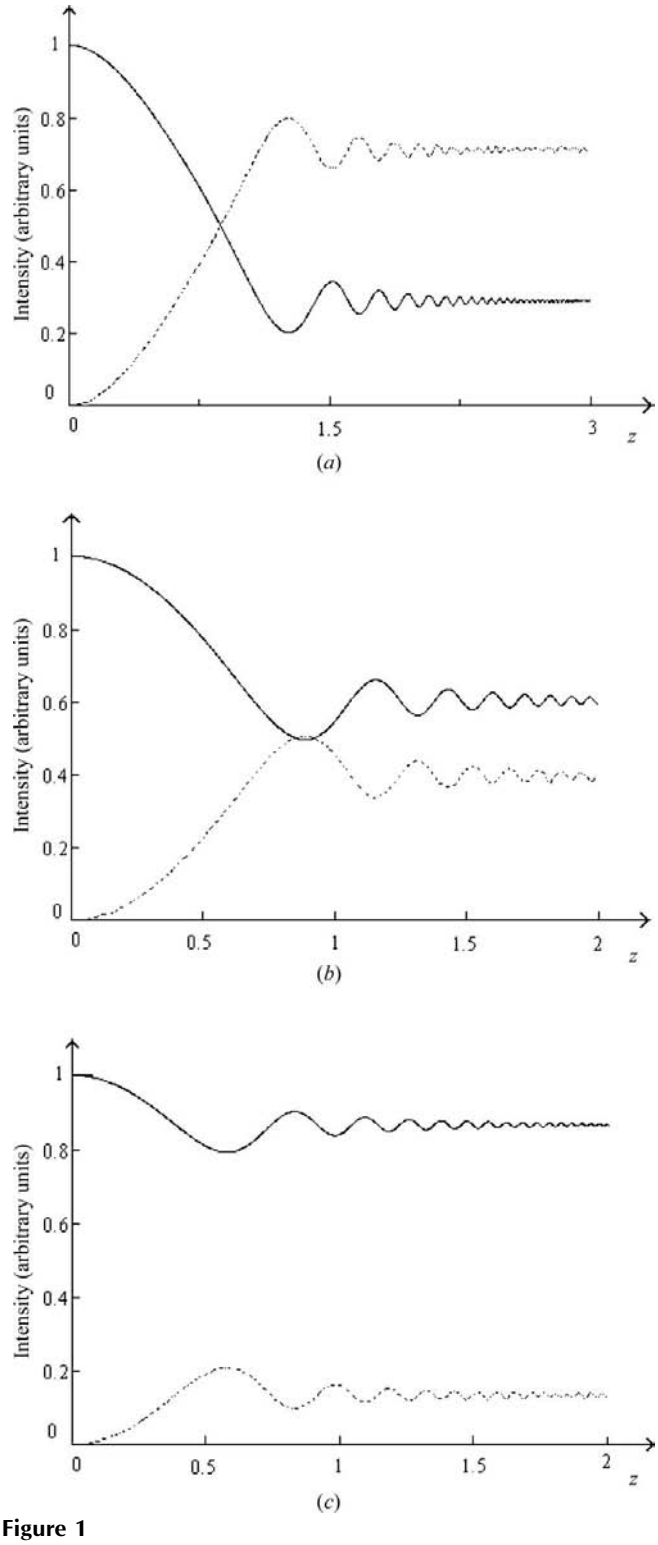

Figure 1
Transmitted (solid line) and diffracted (dotted line) intensities *versus* z (in units of ξ_g/π) for deformation (*a*) $\varepsilon = 1$, (*b*) $\varepsilon = 2$ and (*c*) $\varepsilon = 4$. Departure of the incident wave from Bragg's law $\omega = -2$.

As one can see, oscillation variations with thickness appear in the transmitted and diffracted intensities. The oscillations are complementary; when the transmitted intensity is maximal, the diffracted one is minimal and *vice versa*. It should also be noted that we are interested in studying only the few first oscillations, which are accompanied by appreciable changes of the X-ray intensities and, therefore, can be treated as a dynamical effect. The remaining oscillations fall off rapidly with thickness due to X-ray kinematical diffraction and they tend to the kinematical limit as $z \to \infty$.

Among the numerical results presented here, the most pronounced oscillations are evidently excited for the deformation $\varepsilon = 2$. For weaker deformation ($\varepsilon = 1$) and for stronger deformation ($\varepsilon = 4$) the oscillations are less prominent. In the former case, the into-a-branch scattering is still significant, such that at sufficiently large z the diffracted intensity is greater than the transmitted intensity (see Fig. 1*a*). Meanwhile, the interbranch scattering prevails over the into-a-branch scattering in the latter case, such that the transmitted intensity exceeds the diffracted intensity (see Figs. 1*b* and *c*). This means that the oscillation effect, which is most appreciable for $\varepsilon = 2$, is due to a fragile balance between the interbranch and into-a-branch scattering. Moreover, it is necessary to admit that the oscillations of the X-ray intensities are beyond the conventional range $\Delta z_{\rm D}$ of X-ray dynamical diffraction, which is determined by the condition $(\xi_g/\pi)|q(z)| \lesssim 1$. (For the deformations $\varepsilon = 1$, 2 and 4 the range $\Delta z_{\rm D}$ in units of ξ_g/π is given by the intervals {0.35–0.90}, {0.0–0.55} and {0.0–0.2}, respectively.) Clearly, this fact reflects the interbranch character of the oscillation effect, associated with the interbranch sharp changes of the phase of the X-ray wavefields, which may occur in strongly deformed regions following the range $\Delta z_{\rm D}$. Within the range $\Delta z_{\rm D}$, the conventional *Pendellösung* effect disappears due to the considerable deformations in these cases (see Fig. 1). Nevertheless, the into-a-branch scattering is able to lead to a considerable growth of the diffracted intensity, which is the largest in the case of the deformation $\varepsilon = 1$.

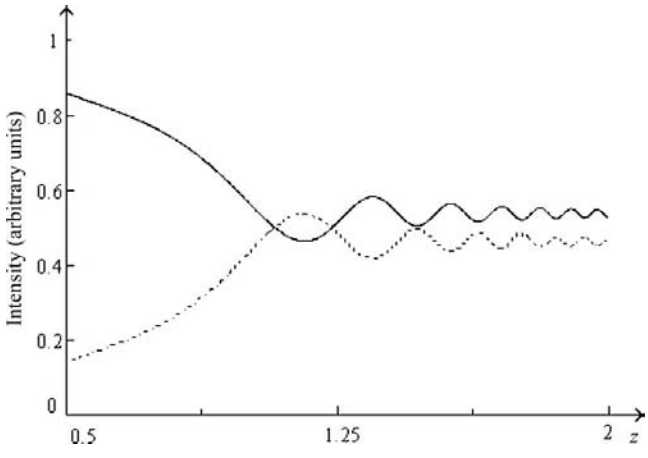

Figure 2
Transmitted (solid line) and diffracted (dotted line) intensities *versus* z (in units of ξ_g/π) for the departure $\omega = -4$ and the deformation $\varepsilon = 2$.

Thus, taking into account that the oscillations considered are out of the range $\Delta z_{\rm D}$ and precede the kinematical features, we will call them transient beating. It is worth paying attention to the fact that the depth of their location also depends on the departure ω. With increasing absolute value of ω, the transient beating is displaced to a more deformed region of the crystal (compare Figs. 1*b* and 2, which correspond to the same deformation but different values of ω). It turns out that this fact will play an important role in the further discussion concerning the practical application of the beating effect to the study of lattice defects.

3. Theoretical aspects of the interbranch transient beating effect

For theoretical study of the diffraction effects originating in the interbranch splitting of the X-ray wavefields, one may apply the 'eikonal' representation of dynamical theory. Then, for the wavefields constituting the transmitted beam, the appropriate fundamental equations have the form

$$\frac{{\rm d}A_0^{1,2}(z)}{{\rm d}z} = -\frac{A_0^{2,1}(z)\exp\{\mp(2i\pi/\xi_g)\int_0^z p(z_1)\,{\rm d}z_1\}}{2p^2(z)[\omega \pm (1+\omega^2)^{1/2}]}\frac{{\rm d}\eta(z)}{{\rm d}z}, \quad (5)$$

where $\eta(z) = \xi_g q(z)/\pi$ and $p(z) = [1+\eta^2(z)]^{1/2}$. The amplitudes $A_0^{1,2}(z)$ are the coefficients of the expansion $D_0(z) = \sum_{j=1,2} A_0^j(z)\Phi_0^j(z)$, where $\Phi_0^{1,2}(z)$ are the eikonal solutions for the transmitted wave of Takagi's equations for the 'upper' and 'lower' dispersion branches, respectively. Equations (5) can be deduced from Takagi's equations by exploiting the variation Lagrange formalism (Shevchenko, 2005). It should be noted that by using equations (5) it is possible to calculate rigorously the contribution of the interbranch scattering to the phase of the X-ray wavefields in the case of strong deformation specified by $\varepsilon \gg 1$. This contribution is most considerable near the point z_0, which is the complex turning point for the eikonal solution. In a highly deformed crystal, the interbranch phase changes may also lead to the 'fine structure' diffraction effects predicted by Shevchenko (2009).

The interbranch splitting of the local dispersion surface can be directly derived from equations (5). Indeed, in the close vicinity of any point z_s, one can approximate the X-ray wavefields by plane waves, such that the solutions of equations (5) have the form

$$A_0^{1,2}(z) = C_{1,2}^{+}(z_s)\exp\{i(Q_s \mp W_s)z\} + C_{1,2}^{-}(z_s)\exp\{i(-Q_s \mp W_s)z\}. \quad (6)$$

Here the value $2Q_s = 2[W_s^2 + (\pi/\Lambda_s)^2]^{1/2}$ determines the interbranch splitting of the local dispersion surface, where the value $\pi/\Lambda_s = \xi_g \mathbf{g}\,\mathbf{u}''(z_s)/[4\pi p^2(z_s)]$ is the interbranch contribution to the splitting at z_s and $W_s = \pi p(z_s)/\xi_g$ is the phase deviation from the interbranch contribution, produced by the into-a-branch scattering. As shown by equations (6), each of the wavefields corresponding to the local dispersion surface splits up into the pairs of 'new' waves specified by the wavevectors $\pm Q_s - W_s$ and $\pm Q_s + W_s$.

The energy distribution between the waves of the transmitted beam can be described with the help of the 'new' Bloch modes $\psi_B^{\pm}(z)$, which in the vicinity of point z_s have the form

$$\psi_B^{\pm}(z) = \exp\{\pm Q_s z\}\big[C_1^{\pm}(z_s)\exp\{-iW_s z\}\Phi_0^1(z) + C_2^{\pm}(z_s)\exp\{iW_s z\}\Phi_0^2(z)\big]. \quad (7)$$

By analogy with conventional X-ray dynamical theory, the expressions (7) for 'new' Bloch modes are appropriate combinations of the waves corresponding to the 'new' upper and lower branches. Taking into account the fact that at the point z_s the eikonal solutions $\Phi_0^{1,2}(z)$ can be approximated by plane waves with the wavevectors $\pm W_s$, respectively, we rewrite equations (7) as

$$\psi_B^{\pm}(z) = \exp\big\{\pm Q_s z\big\}\psi_s^{\pm}, \quad (8)$$

where $\psi_s^{\pm} = C_1^{\pm}(z_s) + C_2^{\pm}(z_s)$ are the amplitudes of the Bloch modes. As shown by expression (8), the 'new' Bloch modes, corresponding to wavevectors $\pm Q_s$, possess local translation symmetry by infinitesimal spacing. Bearing in mind expression (8), one can obtain for the transmitted intensity

$$I_0(z) = \big|\psi_s^{+}\big|^2 + \big|\psi_s^{-}\big|^2 + 2\cos\big\{2Q_s z + \varphi_s\big\}, \quad (9)$$

where $\varphi_s = \arg\{\psi_s^{+}(\psi_s^{-})^{*}\}$. In expression (9), the last term describes the interference of the 'new' Bloch modes, specified by the wavevector Q_s. In this connection, it makes sense to interpret the transient beating as the result of the interference of the 'new' Bloch modes associated with the interbranch splitting of the local dispersion surface. Meanwhile, for a weak distortion, this effect disappears and the conventional *Pendellösung* beating follows from this theory. Substituting the solution (6) into equations (5), we write the ratios for the amplitude $C_{1,2}^{\pm}(z_s)$ to show

$$\frac{C_2^{\pm}(z_s)}{C_1^{\pm}(z_s)} = i\gamma_s^{\pm}\Lambda_s(Q_s \mp W_s), \quad (10)$$

where $\gamma_s^{\pm} = \exp\{(\mp 2i\pi/\xi_g)\int_0^{z_s} p(z)\,\mathrm{d}z\}$. It follows from equations (10) that for a weak deformation (*i.e.* when $W_s \gg \pi/\Lambda_s$), the amplitude $C_2^{+} \ll C_1^{+}$ and $C_1^{-} \ll C_2^{-}$. Then, by neglecting the 'new' waves C_2^{+} and C_1^{-} in solution (6), we reduce the expression for the amplitude $D_0(z)$ to the conventional representation for a two-sheet dispersion surface specified by the wavevectors $\pm\pi p(z_s)/\xi_g$, which are limits of the appropriate values $\pm Q_s$ for a slightly deformed crystal. On the other hand, for large gradient satisfying the condition $\pi/\Lambda_s \gg W_s$, the interbranch transient beating will be absent too. This is due to the interbranch transfer of the energy from the ψ_B^{+} Bloch mode to the ψ_B^{-} mode within the range Δz_D (Shevchenko & Pobydaylo, 2005). As a result, beyond Δz_D $\psi_B^{+} \to 0$ and, consequently, the interference of the 'new' Bloch modes can be neglected. However, in the case of the intermediate deformation $W_s \simeq \pi/\Lambda_s$, a considerable part of the energy does not transfer from the ψ_B^{+} mode to the ψ_B^{-} one within the range Δz_D due to still considerable into-a-branch scattering. Thus, when a balance between the interbranch and into-a-branch scattering happens, the modes $\psi_B^{\pm}$ will have comparable amplitudes beyond Δz_D and, therefore, their interference may be significant in this case.

Table 1
Positions of the interference maxima and minima in units of ξ_g/π of the transmitted intensity I_0 in the case of the deformation $\varepsilon = 2$.

k	$z_{\min}$	z_{2k-1}	$z_{\max}$	z_{2k}
1	0.89	0.78	1.15	1.10
2	1.31	1.28	1.43	1.41
3	1.52	1.50	1.60	1.58
4	1.66	1.65	1.72	1.71
5	1.77	1.76	1.82	1.81

Summing up the phases of the X-ray wavefields, one can obtain the resulting phases of the 'new' Bloch modes at any point z as $\pm\int_0^z Q(z_1)\,\mathrm{d}z_1$ (Shevchenko, 2009). Hence, the positions z_n of the interference features can be calculated from the expression

$$\int_0^{z_n} Q(z_1)\,\mathrm{d}z_1 = (\pi/2)n, \quad (11)$$

where integer $n = 1, 2, 3, \ldots$. Bearing in mind that the cosine function describes interference of the 'new' Bloch modes constituting the transmitted beam, it is natural to suggest that odd numbers n correspond to the minimum of the transmitted intensity, whereas even numbers n correspond to the maximum of the intensity I_0. To verify these considerations, we compare the values z_n obtained from equation (11) with the appropriate $z_{\max}$ and $z_{\min}$ following from the numerical solution of Takagi's equations (2). The results of the calculations for the first five maxima and minima of the intensity I_0 are given in Table 1.

It is obvious that there is a good correlation between the values of $z_{\min}$ and z_{2k-1} and also between $z_{\max}$ and z_{2k}. This fact demonstrates the correctness of the viewpoint presented here of the nature of the beating effect in a strongly deformed crystal. As shown by the table, the period of beating decreases with increasing depth z (*i.e.* with growing local distortions) and it tends to the kinematical value, which does not depend on the extinction length. It should also be noted that the positions of the interference maximum and minimum corresponding to the diffracted wave will be complementary to the interference features of the transmitted wave. This means that odd numbers n satisfying condition (11) will determine the maximum of the diffracted intensity, whereas even numbers n will specify the minimum of the diffracted intensity.

4. Interbranch transient beating induced by an edge dislocation

Interbranch transient beating was shown to be the interference effect owing to a lattice distortion. It is specified by the considerable gradient that causes the interbranch splitting of the local dispersion surface. Moreover, for excitation of the beating, it is necessary that the interbranch contribution to the phase of the X-ray wavefields would be of the order of the into-a-branch contribution. It follows from this that the

interbranch extinction length Λ_g must be comparable with the conventional extinction length ξ_g. [In this connection, see also conditions (1) and (2).] This means that the period of the beating, estimated as the value Λ_g, will have an appreciable magnitude. Therefore, one can suggest that the beating effect may be observed in X-ray topography experiments, which deal with a long-range strain field. A crystal characterized by a sufficiently large value of ξ_g would be preferable for such studies. Taking this into account, we recall the work of Kito & Kato (1974) devoted to the X-ray topography studies of growth of an $NaClO_3$ crystal specified by a small structure factor. It was reported that besides well known *Pendellösung* fringes (Kato, 1963), fringes of an apparently different type are observed in the X-ray patterns. It was also established that they are accompanied by a continuous lattice bending associated with the discreet misorientation at the boundary of the growth sectors. By analogy with the conventional *Pendellösung* fringes, the new fringes were observed to be due to the relevant wedge-shaped growth sectors. Moreover, in the work by Tikhonova (1979), nonconventional oscillations of the X-ray intensities arising in the strongly deformed region were also described for a homogeneously bent crystal. They were treated as a dynamical diffraction effect different from the *Pendellösung* beating.

In a real crystal, continuous deformations are often caused by dislocations. In this case, one can observe the direct image, which is due to the reflection of the X-ray direct beam by the more distorted areas close to the diffraction core (Authier, 1967; Miltat & Bowen, 1975). Assuming an edge dislocation, we would like to discuss the possibility of exciting of interbranch transient beating, which enables the study of details of the direct image. In this connection, it is also worth noting that interference fringes caused by lattice distortions around some defects were observed in resonant scattering X-ray topography for GaAs in the Laue case (Negishi *et al.*, 2007). These defects were suggested by Negishi *et al.* (2004) to be an edge dislocation. Bearing this in mind, we present arguments to support this viewpoint by applying the considerations developed above.

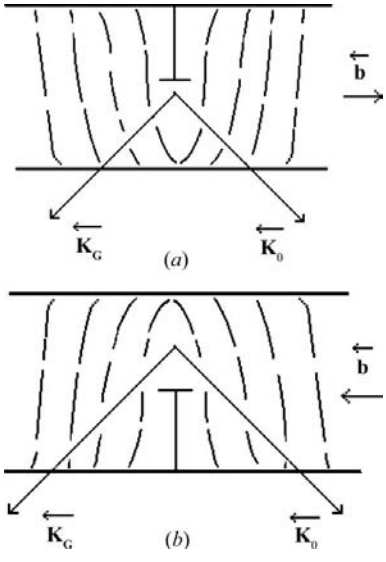

Figure 3
X-ray diffraction in a crystal which contains positive (*a*) and negative (*b*) edge dislocations.

For simplicity, we suppose that a slip plane is oriented parallel to the crystal surface, such that one can distinguish dislocations with different orientations of Burgers vectors (see Figs. 3*a* and *b*). As one can see, the reflecting planes on different sides of the dislocation line deviate from their positions in the perfect crystal in opposite ways. This means that the Bragg condition may be locally satisfied only on one side of the dislocation line, which deviates in the opposite sense relative to the departure ω. Then interbranch scattering may be activated on this side while it will be absent on the other side of the dislocation line.

Thus, in the case of an edge dislocation, the interbranch transient beating may occur only on one side of the dislocation line. Clearly, a change in sign of the dislocation leads to excitation of the beating on the other side of the dislocation line. It should be noted that these facts were experimentally verified in the work by Negishi *et al.* (2007). It was found that around two defects (defined as A and B) the interference fringes arise only on one side of the kinematical image, such that these sides are different for the defects. By suggesting that these fringes are due to the interbranch effect, it is natural to consider such defects as edge dislocations which have opposite signs. Moreover, taking into account the diffraction schemes sketched in Figs. 3(*a*) and (*b*), it is possible to predict as well that contrasts around the defects must be reversed with a change of direction of **g**.

It is necessary to admit that the interbranch transient beating can be directly observed in X-ray plane-wave topography due to the specific character of the strain distribution near the dislocation line. In the given case, the displacement **u** can be approximated by (Hirsh *et al.*, 1977)

$$\mathbf{u} = \mathbf{b}\tan^{-1}\{2(z-y)/x\}, \qquad (12)$$

where y and x are the depth of the location of the dislocation in the crystal and the distance from the dislocation line in the direction parallel to the crystal surface, respectively. It follows from equation (12) that the distorted region which contributes to the interference fringes in the X-ray images is curved. This is shown in Fig. 4, which corresponds to the right-hand side of the region near the dislocation line.

In Fig. 4, the dashed region responsible for the interference fringe is between the two circles expressed by the formulas following from equation (12):

$$(z-y)^2 + \left(x - R_{1,2}\right)^2 = R_{1,2}^2;$$

here $R_{1,2} = b/(2\Delta\Theta_{1,2})$, where $\Delta\Theta_1$ and $\Delta\Theta_2$ ($\Delta\Theta_2 > \Delta\Theta_1$) are the effective misorientations which determine the boundaries of the region of the interbranch beating. It is necessary to take into account that this effect is inherent to the highly distorted region, which in relation to the incident wave is specified by a misorientation greater than the angle $\Delta\psi_{1/2}$, where $\Delta\psi_{1/2}$ is the perfect crystal reflection range. Thus, we can imply that $\Delta\Theta_1 = -\Delta\Theta_i + \Delta\psi_{1/2}$ and $\Delta\Theta_2 =$

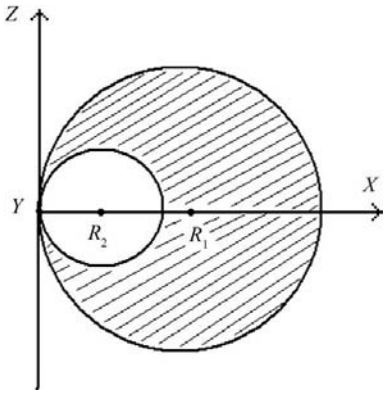

Figure 4
The volume distribution (dashed region) which contributes to the interference fringes.

$-\Delta\Theta_i + K\Delta\psi_{1/2}$, where $\Delta\Theta_i$ ($\Delta\Theta_i < 0$) is the angular departure of the incident wave from Bragg's law and K is a coefficient greater than 1. It specifies the upper limit of the angular range of exciting of the interbranch beating. (The value of K in Fig. 4 is 2.)

Thus, the curved form of the transient beating region makes it possible to observe the fringes in the X-ray pattern. Moreover, it follows from this experiment that the fringe spacing increases as the distance from the defect increases. In other words, the period of the beating decreases when approaching the defect, around which the deformation increases considerably. Clearly, this fact also agrees with the numerical results presented in Table 1, which show a decrease of the period with increasing z, that is to say, with increasing lattice distortions. This property of the beating can also be verified analytically, by taking the limit $z \rightarrow \infty$ in expression (11).

Another feature of the interference fringes around the defects A and B was established by Negishi *et al.* (2007) by analyzing their positions in the X-ray pattern. It turned out that the position of the fringes moves with varying the departure $\Delta\Theta_i$. Obviously, this is similar to displacement of the interbranch oscillations with a change in the value of ω, shown in Fig. 2. In addition, it is necessary to note that we have considered the case of a dislocation parallel to the crystal surface. Assuming such geometry, movement of the fringes will take place only within the region to the side of the dislocation line which corresponds to the appropriate sign of $\Delta\Theta_i$. However, this principle may be violated in the case of some tilt between the crystal surface and the slip plane. In this case, with varying the value of $\Delta\Theta_i$ the Bragg conditions may be locally satisfied on different sides of the image. Therefore, the interbranch fringes may be observed on the right or on the left sides of the image under different values of $\Delta\Theta_i$ which have the same sign.

Thus, the interpretation of interference fringes induced by an edge dislocation as an interbranch effect is in line with the experimental study carried out by resonant scattering X-ray topography. Because this effect occurs in the strongly deformed region which is close to the nucleus of the defect, it can be used for direct determination of the type of the defect and for a local study of a lattice distortion around a defect.

5. Conclusions

Here, we sum up the main results obtained in this work.

(1) Strain-dependent changes of the X-ray intensities are analyzed for the deformations causing the interbranch splitting of the local dispersion surface. It is shown that the interbranch transformation of the local dispersion surface is accompanied by the interbranch oscillations of the intensities of the transmitted and diffracted waves, called transient beating.

(2) It is established that the interbranch transient beating of the X-ray intensities is due to the interference of the 'new' Bloch modes. These modes are responsible for the interbranch redistribution of the energy and they may interfere constructively beyond the dynamical diffraction region.

(3) The period of the transient beating is of the order of the conventional extinction length. Therefore, this effect can be observed in an X-ray topogram and it may be used to specify the structure of a defect. Because the fringes occur in the strongly deformed region close to the defect, they can be considered as 'fine structure' of the direct image.

(4) The experimental study of the interference fringes induced by lattice distributions around defects assumed to be an edge dislocation is discussed. This type of defect is verified by interpreting the fringes as the interbranch beating effect.

The author would like to thank Emeritus Professor André Authier for his useful comments on the manuscript.

References

Authier, A. (1967). *Adv. X-ray Anal.* **10**, 9–31.
Authier, A. (2005). *Dynamical Theory of X-ray Diffraction.* Oxford University Press.
Authier, A. & Balibar, F. (1970). *Acta Cryst.* A**26**, 647–654.
Balibar, F. & Malgrange, C. (1975). *Acta Cryst.* A**31**, 425–434.
Hirsh, P., Howie, A., Nicholson, R., Pashley, D. & Whelan, M. (1977). *Electron Microscopy of Thin Crystals.* New York: Krieger.
Kato, N. (1963). *J. Phys. Soc. Jpn*, **18**, 1785–1791.
Kito, I. & Kato, N. (1974). *J. Cryst. Growth*, **24/25**, 544–548.
Miltat, J. E. A. & Bowen, D. K. (1975). *J. Appl. Cryst.* **8**, 657–669.
Negishi, R., Fakamachi, T., Yoshizaka, M., Hirano, K. & Kawamura, T. (2007). *Phys. Status Solidi A*, **204**, 2694–2699.
Negishi, R., Yoshizawa, M., Zhou, S., Matsumoto, I., Fukamachi, T. & Kawamura, T. (2004). *J. Synchrotron Rad.* **11**, 266–271.
Penning, P. (1966). PhD thesis. Technical University of Delft, The Netherlands.
Penning, P. & Polder, D. (1961). *Philips Res. Rep.* **16**, 419–440.
Shevchenko, M. (2005). *Acta Cryst.* A**61**, 512–515.
Shevchenko, M. (2009). *Acta Cryst.* A**65**, 352–359.
Shevchenko, M. & Pobydaylo, O. (2005). *J. Phys. D Appl. Phys.* **38**, A232–A234.
Tikhonova, E. (1979). *Solid State Phys.* **21**, 1558–1560.